

Integrated SAR /GPS / INS for Target Geolocation Improvement

Michail Papazoglou and Christos Tsioras¹

Abstract.

A big percentage of military men and policy of scientific research aims in the sector of technology of fusion of sensors. However, up to now there has been a little progress in the fusion study of Radar sensors with Synthetic Diaphragm (Synthetic Aperture Radar sensors (SARS)) and Pilotage Sensors. As indicative examples, one can state the sensors of inactive pilotage (Inertial Navigation Sensors (INS)), as well as the systems of world localization (Global Positioning System (GPS)). SARS are used in recognition operations and pursuit. The received SAR scope and measurement rate are processed independently from the system of pilotage.

This work investigates a likely technique for the fusion of information from the pilotage sensors and the measurements of objectives SAR. An incorporated system INS/GPS/SAR is simulated through a Kalman filter, and the SAR profits of geolocation precision objectives are analyzed. Three different models of GPS are used. Each GPS model is incorporated in a common INS/SAR combination aiming at the improvement of geolocation precision objectives. The obtained results show that the pursuit with use of SAR can be strengthened, via the conformity of unification of an INS/GPS pilotage system, without any increase of SAR analysis.

Keywords: Sensors radar of synthetic diaphragm, synthetic aperture radar sensors, sensors of inactive pilotage, inertial navigation sensors, systems of world localization, global positioning system, sensor, radar, radar sensor, pilotage Technology, Kalman filter, filter, simulation, geolocation, fusion

¹ 2nd Lieutenants, Hellenic Army General Staff
E mail addresses: mikepapazg@yahoo.gr and mike88papa@yahoo.gr

1 Introduction

There are four technology areas presented in this paper:

- Inertial Navigation Systems (INS),
- Global Positioning System (GPS),
- Synthetic Aperture Radar (SAR),
- System integration and Kalman Filter.

On these issues, there is already an extensive and exhaustive general Bibliography ([5, 6, 7, 8, 9, 10, 11, 13, 16 and 17]).

The Inertial Navigation System (INS) is using outputs of gyroscopes and accelerometer measurements to provide an independent indication of the position, velocity and attitude of the aircraft in space. Because the operation of an INS performed in inert space, this function is not subject, in theory, to errors associated with the earth's rotation, the dynamics of the aircraft or any other such type effects.

There are two major types of INS implementations: the platform and the strapdown.

A platform INS contains an inertial stabilized platform that uses gimbals to maintain its stability.

A strapdown INS utilizes mathematical algorithms to determinate a computational platform.

The Sensor System of Global Positioning System (GPS) is a constellation of 24 satellites which transmit electromagnetic signals to GPS receivers in the platform of the user. The GPS receiver determines the sequence of use of each satellite from the receiver and from the user. The series provided by the receiver called pseudo-series due to the presence of various erroneous signals.

There are 4 unknown parameters involved with GPS positioning: the three-dimension position parameters (x, y, z) and the GPS time.

Therefore, as long as there are at least four Satellite Vehicles GPS (SV GPS) that are not beyond the scope of supervisory receivers, pseudo-series provided by the GPS satellite vehicles used to determine the user's position relative to the earth.

There are four types of GPS receivers:

- Civil Single Positioning Service (SPS).

- Military receivers account for selective availability (SA) by using decryption techniques.
- Differential Global Positioning Systems (DGPS).
- Carrier Phase Differential GPS (CPGPS).

The geometry of SV GPS plays an important role in determining the location via GPS. Indicatively one “poor” geometry of SV GPS to the receiver can result Geometric “confusion” (Geometric Dilution of Precision (GDOP)) which may create problems in the solvability of the positions of GPS.

One of the widespread recognition sensors are the Synthetic Aperture Radar (SAR). The SAR produces high-resolution images of surface targets and has the ability to operate in all weather conditions. Since it can work even when there are clouds, unlike electrically-optical sensors, thus becoming a key recognition sensor images.

The typical SAR sensors provide two models of operation: the Search and the Spotlight.

In the search function, the SAR radiates over a wide strip of land providing just a picture box (and usually lower-resolution). Mode of viewing the SAR radiates over a strip of land narrower more times to produce a higher resolution image.

The integration of INS and GPS handled properly using a filter Kalman. In this case, the Kalman filter estimates the errors in position derogation INS, the velocity measurements and the mounting space. The filter also estimates the errors in the GPS measurements pseudo-series due to deviations timing distortions in the slope and atmospheric errors. Assuming proper modeling, these errors can be calculated with very high precision. Towards this direction, the detail attribute model, the more reliable model accurately represents the true, the real physical system. These complex models are called “truth models”.

There are different methods of systems integration in navigation systems. The two most typical methods applied are: the “tight” and “loose” integration.

The loose integration method is characterized as " technique per filter aid" (filter - aided - filter). In this case, each sensor navigation system uses the familiar Kalman filter in order to process the measurements. Processed measurements are combined through another Kalman filter to obtain the final consolidated positioning.

The tight method integration of navigation systems combines unprocessed measurements from sensors through a single filter Kalman.

The Kalman filter is an optimal algorithm repeating data. The filter is optimal in the sense that all to the filter available information processed and incorporated. Additionally, the filter is inductive, in the sense that it requires all the previous data items are kept stored and handled reprocessed every time a new measurement is available.

The Kalman filter processes are all available measurements of the variable of interest. Regardless of their accuracy, these procedures are based on:

- knowledge of the system and measuring the strength of this and
- the statistical description of:
 - Noise systems,
 - Measurement error and
 - Uncertainties of models.

A True Model defined as a true model of the variable of interest. The True Model is a result of thorough analysis of the system of interest and our induced similar traits that error. Through this extensive testing can take an extremely accurate representation of the system.

However, still there will be some small amount of error in the model, since the very nature cannot be modeled perfectly. Therefore, a True Model must provide the highest reliability to represent convincingly the “real world”. The True Model for a typical dynamic measurement system can be extremely extensive. A good verification models could include more than 100 situations and precision third or fourth order. For example, the Litton LN-93 Strapdown INS contains 93 statements in the Model truths. Furthermore, a True Model GPS can have up to 30 states. The benefits of a verification models are clear: in a simulation Model Verification will determine the real measurements in the "real world" of a dynamic system. However, due to network (online (online)) restrictions placed on the calculations, these large models become computationally burdensome. Therefore, in most cases, will be used a restricted model Kalman filters to monitor the performance of adequate verification models.

When designing a filter Kalman, for the estimation of false statements, it is important to keep the number of statements to a manageable level.

Typically, the design of the filters should adapt the filters so that the filters can be operated in a limited processing speed, as well as specific memory allocation.

The final result on the web (direct, online) connection Kalman filter is a filter model that tracks the exact Model Verification systems, but has smaller (and therefore more manageable) number of states.

Two steps are important in designing a proper filter model:

- state order reduction
- filter tuning

The first step in designing filter model is the decrease of verification models. This step involves the analysis of the less necessary statements of verification models, either by absorbing them in the existing conditions or eliminating the whole.

Coordination filters offsets the elimination and absorption conditions in the Model Verification. As mentioned previously, in the design of filters intended to return a verification models using a reduced order model of the web (hence direct, online) connection filter.

There are various techniques used for the integration of different sensors sequential. In this paper we present two such techniques: tight integration and loose integration.

Tight completion is defined as the integration of multiple sensors through management unprocessed measurements. A simple Kalman filter is often used during a tight integration to process dynamics and sensor readings. Other types of filters could be used, but the Kalman filter is the best option to combine all the information from the following sensors.

The loose integration includes completion pretreated sensor information. In cases where the existing sensors to be completed (e.g., an aircraft has already an INS or an SAR and comes to a complete GPS), the loose integration techniques may be the only available technique.

There are many array of methods for representing position and velocity of an aircraft with respect to the Earth. A technical representation transformations Coordinate reference systems are Table Cosines Direction (direction cosine matrix (DCM)). The DCM is a computationally efficient method for converting a reference system to another based on a three-dimensional position.

A typical reference system for GPS apps is the reference system earth-centered-earth-fixed (ECEF). This will be the base system for the representation of terrestrial navigation in this session. Following the techniques of Britting and Bagley ([13, 17]), developed three coordinate transformations DCM:

- Inertial – to- ECEF,
- ECEF-to-Navigation,
- ECEF-to-Wander Azimuth.

Inertial – to- ECEF. The inertial reference system is defined by a rectangular frame of reference that is centered on the center of the earth and three axes positioned as follows: one coordinates axes of x and y are in on earth equatorial plane, and the axis of the coordinate z coincides with the axis of the angular velocity of rotation of the earth.

ECEF-to-Navigation. Generally, it does not serve the purpose of air navigation, information on the position to have the pilots (and their aircraft) on the Earth's center. Therefore, the navigation system is used to determine a position on the Earth's surface (: latitude, longitude, and height). The navigation system is defined as a rectangle, clockwise system. Comes from measurements of INS and axes aligned with the North and the East and the vertical direction.

ECEF-to-Wander Azimuth. The azimuth system is a variant of the navigation system. Azimuthally The system, which can then be represented by an index a , coincides with the system platforms when wandering angle a is equal to 0° . The angle wandering is an angle measured between a platform azimuthally wandering and the North. The purpose of the azimuthally component of wandering is to provide suitable solution INS navigation during the flight over the polar regions of the earth. These areas are causing problems in one platform INS because of shifts 180° in latitude.

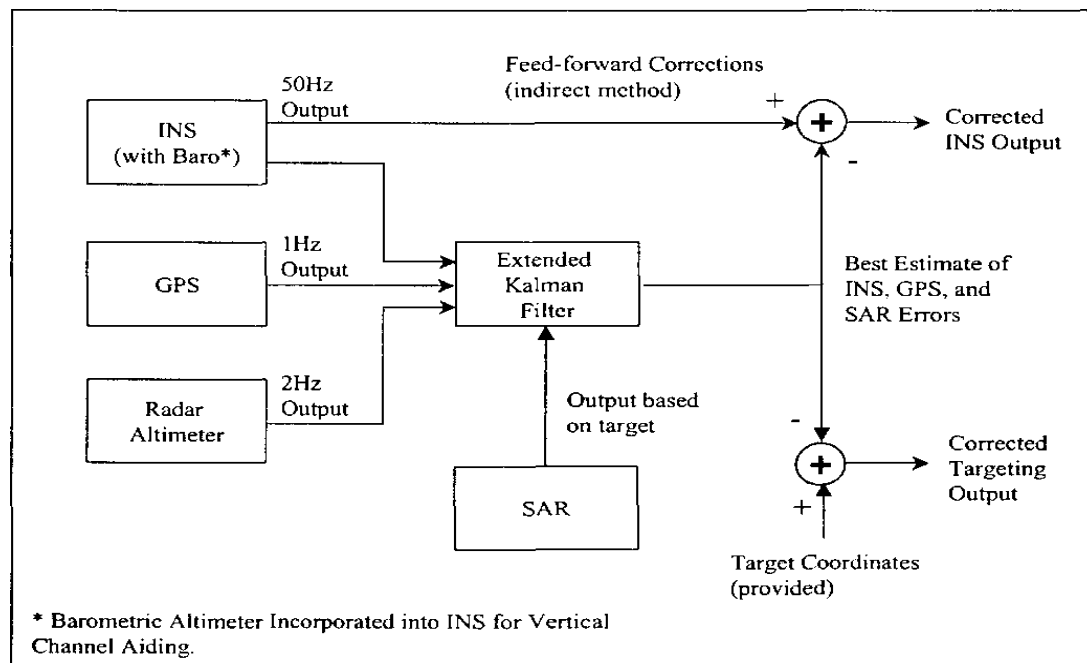
Apart from the above reference systems were presented, there are still three systems, specifically applicable to this Work. The Body Frame, the Computer Frame and System of error angle frame.

2 Modeling Methodology

The following figure describes a top level view of the system integration technique used in this research. A USAF U – 2 reconnaissance aircraft is presented as the airborne platform in which the sensor integration is to be performed. The U -2 supports all three sensors suites:

- The GPS
- The INS
- The SAR reconnaissance sensor.

The GPS measurements are used to update the Kalman filter's estimate of INS position, velocity and attitude errors. These errors are then subtracted from the indicated position, velocity and attitude provided from the INS forming an optimal estimate of the true aircraft position, velocity and attitude.



This research effort focuses on the addition of the SAR model to the existing INS/GPS tight integration. The following model development will allow for the addition of SAR range and range rate measurements into the existing navigation Kalman filter. The navigation filter will be augmented ne several new error states including SAR errors and SAR targeting errors. The coupling of INS/GPS aircraft position errors and SAR targeting errors into a single Kalman filter ill reduce the overall complexity of the system integration and take advantage of the tight integration benefits. It is expected from the research, that a highly accurate aircraft

position and velocity estimate will produce better targeting accuracy without improving the performance of the SAR sensor.

The simulation will be a typical of a U-2 SAR reconnaissance mission. During the U-2 SAR mission, the SAR collection deck is produced prior to aircraft launch. A collection deck provides the order of reconnaissance imagery collection performed during a U-2 SAR mission. The sensor is programmed to take images in both search and spotlight modes throughout the mission at pre-specified locations based on aircraft position. When the U-2 arrives at the proper location, the sensor will image the area in accordance with its collection plan. The INS/GPS position and velocity estimates are provided at an extremely high rate with respect to the SAR measurements. This will provide the highly accurate aircraft position and velocity estimate needed for reducing the SAR targeting error.

To simulate the effect of a highly accurate aircraft position estimate has on SAR targeting errors, three different GPS implementations will be simulated:

- The single,
- The differential,
- The carrier phase.

Each receiver provides measurements to the navigation filter which provides an estimate of the aircraft position, velocity and attitude as well as SAR targeting error. It is expected that a highly accurate GPS will provide a reduction in SAR targeting errors. This particular phenomenon will be analyzed by determining the covariance of the SAR targeting errors to determine how accurate the target position was estimated.

The INS presented in this simulation is a LN-93 strapdown, wander azimuth INS. This model has been used in several simulation research projects and has proven to provide real world characteristics. The following part will outline the model used to represent this INS for the system integration research. Since the INS provides no actual measurements to the navigation Kalman filter, all states associated with the INS, are modeled in the state dynamic matrix. The barometric and radar altimeters augment the INS to account for vertical channel instabilities. The altimeters provide measurements of the aircraft altitude which are accounted for in the navigation Kalman filter.

Litton developed a 93-state error model describing the error characteristics of the LN-93 INS. These error states, represented by the vector $\delta\mathbf{x}$, have been split into 6 different categories:

$$\delta\mathbf{x} = [\delta x_1^T, \delta x_2^T, \delta x_3^T, \delta x_4^T, \delta x_5^T, \delta x_6^T]^T$$

where $\delta\mathbf{x}$ is a 93x1 column vector with the following characteristics:

- δx_1 represents the most often used general error vector containing 13 position, velocity and vertical channel errors.
- δx_2 consists of 16 gyro, accelerometer and baro-altimeter exponentially time-correlated errors, and “trend” states. These states are modeled as first order Markov processes in both the truth model and in the Kalman filter model.
- δx_3 represents gyro bias errors. These 18 states are modeled as random constants in the truth model and are modeled as random walks (with small magnitude pseudonoises) in the Kalman filter.
- δx_4 is composed of the accelerometer bias errors states. These 22 states are modeled in exactly the same manner as the gyro bias states.
- δx_5 depicts accelerometer and initial thermal transients. The 6 thermal transient states are first order Markov processes in the system and Kalman filter.
- δx_6 models the gyro compliance errors. These 18 error states are modeled as biases in the system model and as random walks in Kalman filter.

The INS truth model state space differential equation has the following form:

$$\begin{pmatrix} \delta\dot{x}_1 \\ \delta\dot{x}_2 \\ \delta\dot{x}_3 \\ \delta\dot{x}_4 \\ \delta\dot{x}_5 \\ \delta\dot{x}_6 \end{pmatrix} = \begin{pmatrix} F_{1,1} & F_{1,2} & F_{1,3} & F_{1,4} & F_{1,5} & F_{1,6} \\ 0 & F_{2,2} & 0 & 0 & 0 & 0 \\ 0 & 0 & 0 & 0 & 0 & 0 \\ 0 & 0 & 0 & 0 & 0 & 0 \\ 0 & 0 & 0 & 0 & F_{5,5} & 0 \\ 0 & 0 & 0 & 0 & 0 & 0 \end{pmatrix} \begin{pmatrix} \delta x_1 \\ \delta x_2 \\ \delta x_3 \\ \delta x_4 \\ \delta x_5 \\ \delta x_6 \end{pmatrix} + \begin{pmatrix} w_1 \\ w_2 \\ 0 \\ 0 \\ 0 \\ 0 \end{pmatrix}$$

in which is using the full 93-state truth model.

Negast provides a reduced order truth model, which is reducing the truth model order from 93 to 39-states, using the tuning process. This reduced order truth model is represented by the following equation form:

$$\begin{pmatrix} \delta\dot{x}_1 \\ \delta\dot{x}_2 \\ \delta\dot{x}_3 \\ \delta\dot{x}_4 \end{pmatrix} = \begin{pmatrix} F_{(red)1,1} & F_{(red)1,2} & F_{(red)1,3} & F_{(red)1,4} \\ 0 & F_{(red)2,2} & 0 & 0 \\ 0 & 0 & 0 & 0 \\ 0 & 0 & 0 & 0 \end{pmatrix} \begin{pmatrix} \delta x_1 \\ \delta x_2 \\ \delta x_3 \\ \delta x_4 \end{pmatrix} + \begin{pmatrix} w_1 \\ w_2 \\ 0 \\ 0 \end{pmatrix}$$

The barometric and radar altimeters provide the only measurements from the integrated INS/Altimetre model. The altimeters compensate for the INS's inherent instability in the vertical channel. The altimeter output, ALT_{BARO} , is modeled as the sum of the true altitude h_t , the total error in the barometric altimeter, δh_B , and a random measurement noise V . In order to utilize the difference measurement, the barometric altimeter measurement is differenced with an INS calculated, ALT_{INS} . The INS calculated is the sum of the true altitude and the INS error in vehicle altitude above the referenced ellipsoid, δh . The following difference measurement equation eliminates the unknown true altitude resulting in:

$$\delta z = ALT_{INS} - ALT_{BARO} = [h_t + \delta h] - [h_t + \delta h_B - V] = \delta h - \delta h_B + V$$

The INS error in vehicle altitude above the reference ellipsoid, δh , and total barometric altimeter correlated error, δh_B , are included in the 39-state error model for the INS.

The differenced measurement equation of the radar is similar to the barometric altimeter. Errors in the radar altimeter measurement, ALT_{RALT} , are modeled as white noise (no time correlated component as in the barometric altimeter). Thus, the difference measurement for the radar altimeter is:

$$R_{RALT} = \{[0.01]^2 [AGL_{true} ft]^2\} + 0.25 ft^2$$

The radar altimeter measurement noise covariance, R_{RALT} , is a function of altitude above ground level (AGL), is altitude dependent, and represented by the following equation:

$$R_{RALT} = \{[0.01]^2 [AGL_{true} ft]^2\} + 0.25 ft^2$$

It should be noted that the radar altimeter is modeled to provide altitude measurements after the aircraft drops below 3000 ft AGL. However, the simulated flight trajectory for the U-2 in this research will never drop below the radar altimeter threshold.

The GPS receivers process signals from the GPS satellite constellation to produce a very accurate receiver position. The position is based on the pseudorange measurement from several satellites to the receiver. In this particular research, the GPS receiver has four channels, that means that the receiver can track up to four satellites. It is relatively simple to simulate more channels. However, in doing so, the Kalman filter model and truth model order is increased by four states per channel. For ease of computation and simulation speed, a four channel GPS receiver model provides an adequate representation of the performance of the GPS portion of the INS/GPS/SAR integration. Three different GPS receiver implementations are modeled and will be developed:

- The stand-alone
- The differential
- The carrier-phase

The stand-alone GPS receiver scenario is represented in the following figure. The range between multiple SVs and the receiver is processed into a highly accurate receiver position. However, each SV is subject to many errors that affect the measurement. Atmospheric error, clock errors, satellite position errors, all contribute to an error filled range measurement. As shown in figure, these errors increase or decrease the range distance between the receiver and transmitting satellite. Since the receiver clock can produce a large error in the range between the receiver and satellite is called a “pseudorange”.

The pseudorange provide by the stand-alone GPS receiver is the sum of the true range from satellite to receiver plus errors, including random measurement noise. The following equation shows the total calculation of the GPS filter pseudorange measurement:

$$R_{GPS} = R_{t_j} + \delta R_{cl} + \delta R_{trop_j} + \delta R_{ion_j} + \delta R_{Sclk_j} + \delta R_{Uclk_j} - V_j$$

where $j = 1,2,3,4$ for each SV. Since the true range R_t from SV to receiver can never be measured perfectly, a difference measurement is performed to eliminate this term. This difference measurement is formulated by calculating a “range” from the INS position and the ephemeris provided satellite position, and subtracting the INS

range from the GPS pseudorange. The INS range R_{INS} can be calculated as shown below:

$$R_{INS} = |X_U - X_S| = \left| \begin{pmatrix} x_U \\ y_U \\ z_U \end{pmatrix}^e - \begin{pmatrix} x_S \\ y_S \\ z_S \end{pmatrix}^e \right|$$

where X_U is the aircraft position as provided by the INS and X_S is the SV position. The INS range can also be represented by the following form:

$$R_{INS} = \sqrt{(x_U - x_S)^2 + (y_U - y_S)^2 + (z_U - z_S)^2}$$

Differential positioning GPS (DGPS) is slightly more complex than the stand-alone GPS. The following figure shows the DGPS positioning technique using an accurate surveyed position for the location of the ground based receiver. This reference receiver processes the pseudorange data from all available satellites. The ground receiver usually contains highly accurate clocks which reduce the user clock errors. Since the ground receiver's position is precisely known and its own clock errors are extremely small, each SV's position, clock and atmospheric errors become observable in the pseudorange measurement. This allows the ground receiver to estimate the errors associated with each SV very precisely. The estimates of the SV errors are called differential corrections and can be transmitted from the ground receiver to an airborne DGPS receiver. The airborne receiver will use the differential corrections to remove the proper errors from its own pseudorange measurement. There are few assumptions that are critical to modeling this DGPS technique. First, it is assumed that the airborne receiver has access to the same satellites as the ground based receiver. Second, it is assumed for modeling purposes that the differential corrections are all timed correctly to correspond to the right airborne pseudorange measurement. Last but not least, when processing DGPS measurements, it is assumed that the differential corrections have been applied to the raw pseudorange measurements from the airborne receiver. During standoff reconnaissance missions, like those typically flown by the U-2, these assumptions can be properly invoked as the aircraft will likely fly near a differential transmitter.

The Differential GPS (DGPS) error model is fabricated almost exactly as the stand-alone GPS error model. The first difference is the removal of the SV clock error through differential corrections. A second difference is the absorption of the receiver code loop error into the noise variance in the pseudorange measurement. This leaves

the user clock errors, atmospheric errors and satellite position errors which comprise a 22-state DGPS truth model. However, only the user clock errors retain the same characteristics as the stand-alone GPS model.

The j-satellite specific atmospheric and position DGPS error models are slightly different than the stand-alone GPS model. All truth model DGPS error sources are modeled using the following state differential equations, initial covariances, and zero mean, white noise components:

$$\begin{pmatrix} \delta \dot{R}_{trop} \\ \delta \dot{R}_{ion} \\ \delta \dot{x}_{SVj} \\ \delta \dot{y}_{SVj} \\ \delta \dot{z}_{SVj} \end{pmatrix} = \left[\begin{pmatrix} 1 & 0 & 0 & 0 & 0 \\ 0 & 1 & 0 & 0 & 0 \\ 0 & 0 & 0 & 0 & 0 \\ 0 & 0 & 0 & 0 & 0 \\ 0 & 0 & 0 & 0 & 0 \end{pmatrix} \begin{pmatrix} -(1/500) \\ -(1/1500) \\ 0 \\ 0 \\ 0 \end{pmatrix} \right] \begin{pmatrix} \delta R_{trop} \\ \delta R_{ion} \\ \delta x_{SVj} \\ \delta y_{SVj} \\ \delta z_{SVj} \end{pmatrix} + \begin{pmatrix} w_{trop} \\ w_{ion} \\ 0 \\ 0 \\ 0 \end{pmatrix},$$

$$P_{GPS}(t_0) = \begin{bmatrix} \begin{pmatrix} 1 & 0 & 0 & 0 & 0 \\ 0 & 1 & 0 & 0 & 0 \\ 0 & 0 & 1 & 0 & 0 \\ 0 & 0 & 0 & 1 & 0 \\ 0 & 0 & 0 & 0 & 1 \end{pmatrix} \begin{pmatrix} 1.00ft^2 \\ 1.00ft^2 \\ 0.35ft^2 \\ 0.35ft^2 \\ 0.35ft^2 \end{pmatrix} \end{bmatrix}$$

$$E[w_{GPS}(t)w_{GPS}(t + \tau)] = \begin{pmatrix} 1 & 0 & 0 & 0 & 0 \\ 0 & 1 & 0 & 0 & 0 \\ 0 & 0 & 0 & 0 & 0 \\ 0 & 0 & 0 & 0 & 0 \\ 0 & 0 & 0 & 0 & 0 \end{pmatrix} \begin{pmatrix} 0.0010ft^2/sec \cdot \delta(\tau) \\ 0.0004ft^2/sec \cdot \delta(\tau) \\ 1.0000ft^2/sec \cdot \delta(\tau) \\ 1.0000ft^2/sec \cdot \delta(\tau) \\ 1.0000ft^2/sec \cdot \delta(\tau) \end{pmatrix}$$

The three equations above correlate back to a specific j-satellite. Coupled with the two user clock states, four sets of the equations above (for 4 SVs) provides a total of 22 DGPS error states.

Like the stand-alone GPS pseudorange measurement, the DGPS pseudorange measurement equation is modeled as:

$$R_{DGPS} = R_t + \delta R_{trop} + \delta R_{ion} + \delta R_{Uclk} - V$$

where all differential corrections have been applied and v is zero-mean white Gaussian measurement noise. In order to use the difference measurement technique, the previous equation is subtracted from the INS calculated range to form the truth model DGPS difference measurement:

$$\begin{aligned}
\delta Z_{PR_j} &= R_{INS_j} - R_{DGPS_j} \\
&= -\left[\frac{x_S - x_U}{|R_{INS}|}\right] \delta x_U - \left[\frac{y_S - y_U}{|R_{INS}|}\right] \delta y_U - \left[\frac{z_S - z_U}{|R_{INS}|}\right] \delta z_U + \\
&\quad + \left[\frac{x_S - x_U}{|R_{INS}|}\right] \delta x_S + \left[\frac{y_S - y_U}{|R_{INS}|}\right] \delta y_S + \left[\frac{z_S - z_U}{|R_{INS}|}\right] \delta z_S \\
&\quad - \delta R_{trop_j} - \delta R_{ion_j} - \delta R_{Uclk} + V.
\end{aligned}$$

Note that multipath error is not included in the DGPS measurement model. Multipath noise is generated when reflected GPS signals are processed in the GPS receiver. Normally this noise is very small and can be assumed within the measurement noise. However, when differential corrections are applied, the multipath noise can become one of the most dominant error sources. Since the U-2 receiver is at a considerable altitude, 65000 ft, it is assumed that the multipath noise would primarily affect the differential reference receiver. In this research, the multipath is assumed to be covered within the receiver measurement noise, V .

The carrier phase GPS model presented here follows the development of Bohenek using floating ambiguity resolution. Unlike single and differential GPS, the carrier phase GPS receiver does not process the GPS signal into a pseudorange. A carrier phase measurement is the result of subtracting the generated carrier signal of the receiver from the carrier signal transmitted by a specific GPS satellite. The subtraction of these signals produces a phase range, also known as the carrier phase observable. The carrier phase observable equation is:

$$\Phi = -f(dT - dt) - \frac{f}{c}(R_t - d_{ion} + d_{trop})$$

where: f is the frequency of carrier signal,

dT is the transmission time offset from true GPS time,

dt is the user clock offset from true GPS time,

R_t is the true range from receiver to satellite,

d_{ion} is the range equivalent of ionospheric delay,

d_{trop} is the range equivalent of tropospheric delay and

c is the speed of light.

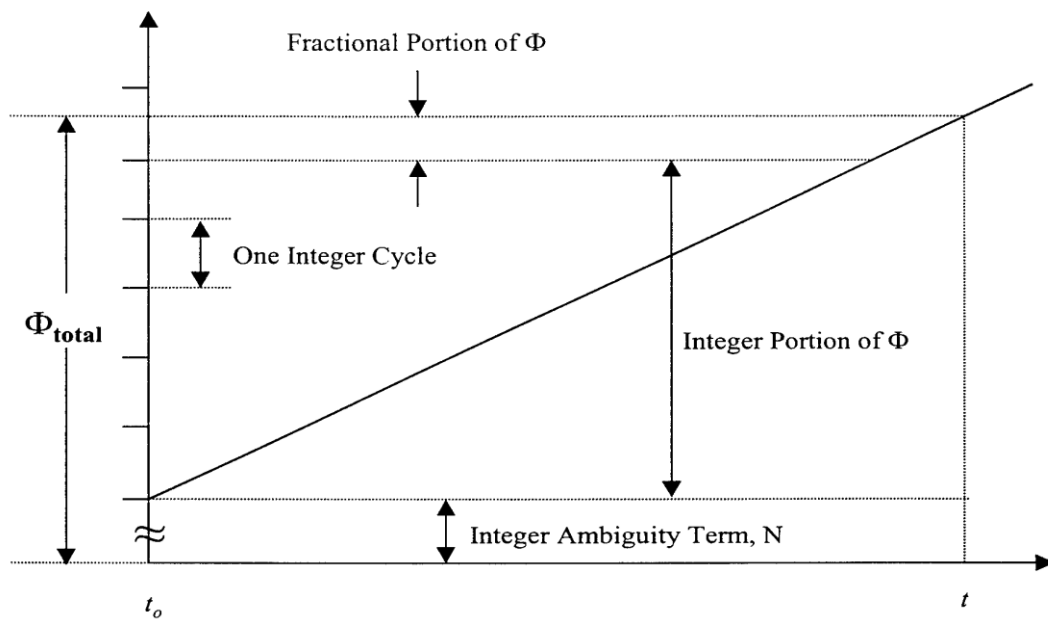
The carrier phase measurement is the measurement of the phase shift between the satellite generated carrier signal and the receiver generated carrier signal. The

phase shift represents a fraction of the total carrier frequency wavelength, so the total phase range measurement between the receiver and the satellite is:

$$\Phi_{total}(t) = \Phi_{frac}(t) + \Phi_{int}(t, t_0) + N(t_0)$$

where $\Phi_{frac}(t)$ is the fraction of total wavelength, $\Phi_{int}(t, t_0)$ is the integer number of phase cycles from the initial reception time to the current time, and $N(t_0)$ is the integer phase ambiguity term. $N(t_0)$ is the difference between the true integer count at the initial time and the current integer count at t_0 measured or calculated by the receiver. The following figure describes the relationship between each facet of the carrier phase measurement. As shown in figure, the total phase range is equal to the integer ambiguity, integer portion of phase range, and fractional portion of phase range.

Assuming that the Φ term is the measured phase observation, it can be represented as the sum of the fraction and integer phase observations (Φ_{frac} and Φ_{int}).



Therefore, the total phase range can be written as the sum of the measured phase observation and the integer ambiguity term, $N(t)$. The measured phase range for the carrier phase observable is shown by the following equation:

$$\Phi_{measured}(t) = -f(dT - dt) - \frac{f}{c}(R_t - d_{ion} + d_{trop})$$

which is the measured phase range in carrier cycles. To convert to feet, you must multiply the previous equation with the carrier wavelength λ , which provides the following form:

$$\Phi(t) = R_t + c(dT - dt) + d_{ion} - d_{trop} + \lambda N(t)$$

When the signal between the carrier phase receiver and the satellite is lost it is called a cycle slip. During this loss the receiver cannot count the integer phase cycles. As a result of this, the receiver may lock onto the wrong integer phase cycle causing the receiver to lose signal lock.

Carrier phase GPS (CPGPS) receivers are generally differential receivers as well. This means that the airborne CPPS receiver has access to differential corrections that can eliminate several error sources. The error model equations for the CPGPS model are similar to the differential GPS model with the addition of the integer ambiguity error. These new states are added to the existing differential states in the following manner:

$$\begin{pmatrix} \delta \dot{R}_{N_1} \\ \delta \dot{R}_{N_2} \\ \delta \dot{R}_{N_3} \\ \delta \dot{R}_{N_4} \end{pmatrix} = \begin{bmatrix} 0 & 0 & 0 & 0 \\ 0 & 0 & 0 & 0 \\ 0 & 0 & 0 & 0 \\ 0 & 0 & 0 & 0 \end{bmatrix} \begin{pmatrix} \delta R_{N_1} \\ \delta R_{N_2} \\ \delta R_{N_3} \\ \delta R_{N_4} \end{pmatrix} + \begin{pmatrix} w_1 \\ w_2 \\ w_3 \\ w_4 \end{pmatrix}$$

with initial state covariance

$$P_{GPS}(t_0) = \begin{pmatrix} 1 & 0 & 0 & 0 \\ 0 & 1 & 0 & 0 \\ 0 & 0 & 1 & 0 \\ 0 & 0 & 0 & 1 \end{pmatrix} \begin{pmatrix} 13ft^2 \\ 13ft^2 \\ 13ft^2 \\ 13ft^2 \end{pmatrix}$$

The ambiguity states are modeled as random biases as long as there are no cycle slips. In addition to that, the $13ft$ value for the initial state covariance is used under the assumption that initially, the CPGPS measurement is only as accurate as a typical differential GPS receiver and has the access to code measurements.

The measurement model for the CPGPS measurements is different than that of the differential GPS model. Since the CPGPS receiver must account for the integer ambiguity term, $N(t)$, an additional error in the range measurement is produced, δR_N . In order for the ambiguity term to become observable in the CPGPS measurement equations, the “double differencing” technique is applied. The double differencing is between the airborne receiver and two separate satellites. This method subtracts a between receiver single difference measurement with another between-receiver single difference measurement using the same receiver and two different satellites to produce the following equation:

$$\nabla\Delta R^{i,j} = R_t^{i,j} - \nabla\Delta R_{ion}^{i,j} + \nabla\Delta R_{trop}^{i,j} + \nabla\Delta R_N^{i,j} + \nabla\Delta V^{i,j}$$

where i and j represent the two different satellites.

The carrier phase range measurement is represented by following form:

$$R_{CPGPS} = R_t - \delta R_{Uclk} - \delta R_{ion} + \delta R_{trop} + \delta R_N + V$$

where the term δR_N represents the range equivalent of the cycle ambiguity term. The previous equation represents one of the single difference measurements. The “between-satellites” single difference transforms the previous equation into:

$$\nabla\Delta R^{i,j} = R_t^{i,j} - \nabla\Delta R_{ion}^{i,j} + \nabla\Delta R_{trop}^{i,j} + \nabla\Delta R_N^{i,j} + \nabla\Delta V^{i,j}.$$

The measurement noise term, $V^{i,j}$, is now doubled ($2 \times E[V^2]$) under the assumption that the satellite measurements are independent of each other. With four satellites, the i/j combinations are: 1 and 4, 2 and 4, and 3 and 4 using satellite 4 as the base satellite. The INS computed “between- satellites” range is:

$$\nabla\Delta R_{INS}^{i,j} = \nabla R_t^{i,j} - A\delta X_U - B\delta Y_U - C\delta Z_U + A\nabla\delta X_S^{i,j} + B\nabla\delta Y_S^{i,j} + C\nabla\delta Z_S^{i,j},$$

where:

- $A = \left[\frac{X_S^i - X_U}{|R_{INS}^i|} \right] - \left[\frac{X_S^j - X_U}{|R_{INS}^j|} \right],$
- $B = \left[\frac{Y_S^i - Y_U}{|R_{INS}^i|} \right] - \left[\frac{Y_S^j - Y_U}{|R_{INS}^j|} \right],$
- $C = \left[\frac{Z_S^i - Z_U}{|R_{INS}^i|} \right] - \left[\frac{Z_S^j - Z_U}{|R_{INS}^j|} \right].$

This method eliminates the user clock bias terms which dominate the SGPS and DGPS models. This will result in a 2-state decrease in the CPGPS truth and filter models.

The Synthetic Aperture Radar (SAR) is one of the most common imaging sensors in the USAF. The primary function of a military SAR sensor is to generate high resolution radar images of ground terrain and ground targets. The two basic measurements a SAR provides are, range and range rate to a target. The SAR range is defined:

$$r = \frac{cT}{2}$$

where T is the transmit time of the transmitted pulse (from transmit to receipt) and c is the speed of light. Range rate is defined by the following form:

$$\dot{r} = \frac{cF_d}{2F}$$

where F_d is the Doppler frequency shift and F is the frequency of the SAR. Using these two basic equations, the SAR error models can be developed for use in the integrated Kalman filter.

Generally, a SAR contains a wide beam antenna which illuminates a large area on the ground. The SAR transmits a radar pulse and samples the magnitude and phase of the return signal. Since radar waves propagate at nearly a constant speed in the Earth's atmosphere, the earliest samples correspond to the points on the ground nearest the aircraft. Likewise the return from more distant points are represented by later samples. The data samples are stored in vectors referred to as range bins. Then these range bins are processed into ground images using the magnitude and phase characteristics of each received pulse. The term synthetic aperture is used because the aircraft utilizes the motion of the aircraft to synthesize the effect of a large aperture antenna from a physically small aperture antenna. Since aperture size is directly correlated with SAR resolution, the larger the aperture, the higher the SAR resolution is. Therefore, a SAR capable of creating a large synthetic aperture can achieve significant resolution increases while maintaining a physical radar aperture that is much smaller. The resolution distance ρ_α , capable from a SAR is directly related to the slant range interval, ΔR , the radar signal speed, c , and the velocity of the aircraft, V , as shown:

$$\frac{2\Delta R}{\rho_\alpha} = \frac{V}{c}$$

For ground mapping, a small resolution distance provides high imagery resolution resulting in better ground targeting.

As with the INS and GPS sensors, SAR measurements contain several errors. The most prominent error in SAR measurements is due to aircraft velocity errors. Since SAR uses the velocity of the aircraft to create the synthetic aperture antenna, incorrect interpretation of the aircraft velocity vector can cause problems recording the Doppler shift of the range measurement over time. Therefore, range rate measurements from SAR must be a function of the aircraft velocity errors.

As with INS, GPS and altimeter models, a SAR error model is developed to determine the errors present in the SAR range and range rate measurements. These SAR error states are included in the extended Kalman filter along with the INS and

GPS error states. The first three states to be included in the Kalman filter are the target position error states: δx_t , δy_t , δz_t . *These states define the amount of SAR targeting error in each SAR range and range rate measurement. Using all the information in the Kalman filter, the bottom line performance of the integrated system is determined through analysis of the target position error states.*

The errors inherent in the SAR itself can cause problems with the range and range rate measurements. First, there are two range measurement errors modeled: the range clock error δr_{CL} , and radar wave propagation speed error δC . The range clock error is defined as the error in the SAR clock. The SAR clock is responsible for keeping track of the transmit and return time of a radar signal. Any errors associated with drifting clock rate or bias effects can cause a delay in the transmit or return time, thus creating a small error in the range measurement. Radar wave propagation speed is needed to map the measured radar wave transmit time to a range measurement. Any error in the radar wave propagation speed can have a “scale factor” type effect on the range and range rate measurement. These two errors are modeled as random biases with the following characteristics:

$$\begin{pmatrix} \delta r_{CL} \\ \delta C \end{pmatrix} = \begin{pmatrix} 0 & 0 \\ 0 & 0 \end{pmatrix} \begin{pmatrix} \delta r_{CL} \\ \delta C \end{pmatrix}$$

with initial covariance values of

$$P_{SAR_1}(t_0) = \begin{pmatrix} 1 & 0 \\ 0 & 1 \end{pmatrix} \begin{pmatrix} 0.01ft \\ 10PPM \end{pmatrix}.$$

The SAR range rate measurement has similar characteristics as the range measurement. First, since the radar measures range rate through the Doppler frequency of return pulses, any frequency shifts in the pulses will cause some bias errors. These frequency shift errors induced through the SAR system and defined as a Doppler shift error δr_D . The radar wave propagation speed error δC can also effect the range rate measurement. The last error source is the frequency error δF . Errors in the frequency of the radar will impact the SAR range rate measurement. The range rate errors are modeled as random biases with the following characteristics:

$$\begin{pmatrix} \delta r_D \\ \delta C \\ \delta F \end{pmatrix} = \begin{pmatrix} 0 & 0 & 0 \\ 0 & 0 & 0 \\ 0 & 0 & 0 \end{pmatrix} \begin{pmatrix} \delta r_D \\ \delta C \\ \delta F \end{pmatrix}$$

with initial covariance values of

$$P_{SAR_2}(t_0) = \begin{pmatrix} 1 & 0 & 0 \\ 0 & 1 & 0 \\ 0 & 0 & 1 \end{pmatrix} \begin{pmatrix} 0.001 \text{ ft/sec} \\ 10\text{PPM} \\ 20\text{PPM} \end{pmatrix}.$$

The total SAR truth model error state differential equation used, is shown in the following equation and includes all SAR errors as well as the SAR targeting errors:

$$\begin{pmatrix} \delta \dot{r}_{CL} \\ \delta \dot{r}_D \\ \delta \dot{C} \\ \delta \dot{F} \\ \delta \dot{x}_t \\ \delta \dot{y}_t \\ \delta \dot{z}_t \end{pmatrix} = \begin{pmatrix} 0 & 0 & 0 & 0 & 0 & 0 & 0 \\ 0 & 0 & 0 & 0 & 0 & 0 & 0 \\ 0 & 0 & 0 & 0 & 0 & 0 & 0 \\ 0 & 0 & 0 & 0 & 0 & 0 & 0 \\ 0 & 0 & 0 & 0 & 0 & 0 & 0 \\ 0 & 0 & 0 & 0 & 0 & 0 & 0 \\ 0 & 0 & 0 & 0 & 0 & 0 & 0 \end{pmatrix} \begin{pmatrix} \delta r_{CL} \\ \delta r_D \\ \delta C \\ \delta F \\ \delta x_t \\ \delta y_t \\ \delta z_t \end{pmatrix} + \begin{pmatrix} 0 \\ 0 \\ w_1 \\ w_1 \\ 0 \\ 0 \\ 0 \end{pmatrix}$$

A nominal initial covariance of 100-ft per channel was provided to each of the SAR targeting errors states.

The SAR measurement model is also developed along the same lines as the INS and GPS models. The SAR range and range rate measurements are integrated into the Kalman filter using the difference measurement technique. An INS calculated range and range rate provides the second measurement type to be subtracted from the SAR measured range and range rate. The SAR range measurement is defined as the true range to the target plus the range errors and measurement noise:

$$r_{SAR} = r_{tar} + \delta r_{CL} + r \delta C + V_r$$

where r_{SAR} defined as the range from SAR to target (r is defined as the range from aircraft to target as opposed to the R which was the range from aircraft to GPS satellite). The SAR range rate measurement is defined as the true range rate from the aircraft to the target plus the range rate errors and measurement noise:

$$\dot{r}_{SAR} = \dot{r}_{tar} + \delta \dot{r}_D + \dot{r} \delta C + \dot{r} \delta F + V_r$$

where V is the range rate measurement noise.

Assuming the target position has been pre-determined, the INS indicated range to the target is defined as:

$$r_{INS_{tar}} = \sqrt{(x_U - x_{tar})^2 + (y_U - y_{tar})^2 + (z_U - z_{tar})^2}$$

Since this particular equation is nonlinear, a Taylor series expansion is performed to generate a first order linear equation in terms of the aircraft and target position error states:

$$r_{INS_j} = r_{true_{tar}} - \left[\frac{x_{tar} - x_U}{|R_{INS}|} \right] \delta x_U - \left[\frac{y_{tar} - y_U}{|R_{INS}|} \right] \delta y_U - \left[\frac{z_{tar} - z_U}{|R_{INS}|} \right] \delta z_U +$$

$$+ \left[\frac{x_{tar} - x_U}{|R_{INS}|} \right] \delta x_t + \left[\frac{y_{tar} - y_U}{|R_{INS}|} \right] \delta y_t + \left[\frac{z_{tar} - z_U}{|R_{INS}|} \right] \delta z_t.$$

The SAR range difference measurement is form as shown below:

$$\begin{aligned} \delta z_{SAR_r} &= r_{INS} - r_{SAR} \\ &= - \left[\frac{x_{tar} - x_U}{|R_{INS_{tar}}|} \right] \delta x_U - \left[\frac{y_{tar} - y_U}{|R_{INS_{tar}}|} \right] \delta y_U - \left[\frac{z_{tar} - z_U}{|R_{INS_{tar}}|} \right] \delta z_U + \\ &\quad + \left[\frac{x_{tar} - x_U}{|R_{INS_{tar}}|} \right] \delta x_{tar} + \left[\frac{y_{tar} - y_U}{|R_{INS_{tar}}|} \right] \delta y_{tar} + \left[\frac{z_{tar} - z_U}{|R_{INS_{tar}}|} \right] \delta z_{tar} \\ &\quad - \delta r_{CL} - r \delta C - V_r. \end{aligned}$$

The previous equation represents the truth model description of the measurement used in the integrated Kalman filter.

The range rate difference measurement is much more complex than the range difference measurement. In order to provide an INS indicated range rate, we use the following form:

$$\dot{r}_{INS_{tar}} = T_{INS_{tar}} / r_{INS_{tar}}$$

where

$$T_{INS_{tar}} = [(x_U - x_{tar})\dot{x}_U + (y_U - y_{tar})\dot{y}_U + (z_U - z_{tar})\dot{z}_U].$$

In order to produce the INS indicated range rate approximation in terms of the error state variables, we use a Taylor expansion. The Taylor expansion is shown below:

$$\begin{aligned} \dot{r}_{INS_t} &= \dot{r}_{tar} + \left. \frac{\partial \dot{r}_{INS_{tar}}(X_{tar}, X_U, \dot{X}_U)}{\partial X_t} \right|_{(X_{tar}, X_U, \dot{X}_U)_{nom}} \delta X_{tar} \\ &\quad + \left. \frac{\partial \dot{r}_{INS_{tar}}(X_{tar}, X_U, \dot{X}_U)}{\partial X_U} \right|_{(X_{tar}, X_U, \dot{X}_U)_{nom}} \delta X_U \end{aligned}$$

$$+ \left. \frac{\partial \dot{r}_{INS_{tar}}(X_{tar}, X_U, \dot{X}_U)}{\partial \dot{X}_U} \right|_{(X_{tar}, X_U, \dot{X}_U)_{nom}} \delta \dot{X}_U$$

where the expected $\delta \dot{X}_{tar}$ term equals zero since the target is not moving (assumption). The INS calculated range from aircraft to target is the following:

$$\begin{aligned} \dot{r}_{INS_{tar}} &= \dot{r}_{tar} + [(r_{INS_{tar}}^{-1})\dot{x}_U - (r_{INS_{tar}}^{-3/2})T_{INS_{tar}}(x_U - x_{tar})]\delta x_U \\ &+ [(r_{INS_{tar}}^{-1})\dot{y}_U - (r_{INS_{tar}}^{-3/2})T_{INS_{tar}}(y_U - y_{tar})]\delta y_U \\ &+ [(r_{INS_{tar}}^{-1})\dot{z}_U - (r_{INS_{tar}}^{-3/2})T_{INS_{tar}}(z_U - z_{tar})]\delta z_U \\ &+ (r_{INS_{tar}}^{-1})(x_U - x_{tar})\delta \dot{x}_U \\ &+ (r_{INS_{tar}}^{-1})(x_U - x_{tar})\delta \dot{y}_U \\ &+ (r_{INS_{tar}}^{-1})(x_U - x_{tar})\delta \dot{z}_U \\ &- [(r_{INS_{tar}}^{-1})\dot{x}_U - (r_{INS_{tar}}^{-3/2})T_{INS_{tar}}(x_U - x_{tar})]\delta x_{tar} \\ &- [(r_{INS_{tar}}^{-1})\dot{y}_U - (r_{INS_{tar}}^{-3/2})T_{INS_{tar}}(y_U - y_{tar})]\delta y_{tar} \\ &- [(r_{INS_{tar}}^{-1})\dot{z}_U - (r_{INS_{tar}}^{-3/2})T_{INS_{tar}}(z_U - z_{tar})]\delta z_{tar} \end{aligned}$$

Using the difference measurement technique we have the following equation:

$$\begin{aligned} \delta z_{SAR_r} &= \dot{r}_{INS_{tar}} - \dot{r}_{SAR} \\ &= \dot{r}_{tar} + [(r_{INS_{tar}}^{-1})\dot{x}_U - (r_{INS_{tar}}^{-3/2})T_{INS_{tar}}(x_U - x_{tar})]\delta x_U \\ &+ [(r_{INS_{tar}}^{-1})\dot{y}_U - (r_{INS_{tar}}^{-3/2})T_{INS_{tar}}(y_U - y_{tar})]\delta y_U \\ &+ [(r_{INS_{tar}}^{-1})\dot{z}_U - (r_{INS_{tar}}^{-3/2})T_{INS_{tar}}(z_U - z_{tar})]\delta z_U \\ &+ (r_{INS_{tar}}^{-1})(x_U - x_{tar})\delta \dot{x}_U \\ &+ (r_{INS_{tar}}^{-1})(x_U - x_{tar})\delta \dot{y}_U \\ &+ (r_{INS_{tar}}^{-1})(x_U - x_{tar})\delta \dot{z}_U \\ &- [(r_{INS_{tar}}^{-1})\dot{x}_U - (r_{INS_{tar}}^{-3/2})T_{INS_{tar}}(x_U - x_{tar})]\delta x_{tar} \\ &- [(r_{INS_{tar}}^{-1})\dot{y}_U - (r_{INS_{tar}}^{-3/2})T_{INS_{tar}}(y_U - y_{tar})]\delta y_{tar} \\ &- [(r_{INS_{tar}}^{-1})\dot{z}_U - (r_{INS_{tar}}^{-3/2})T_{INS_{tar}}(z_U - z_{tar})]\delta z_{tar} \\ &- \delta r_D - \dot{r}\delta C - \dot{r}\delta F - V_r. \end{aligned}$$

The following equation describes the augmentation of each sensor truth model into a single Kalman filter dynamics equation:

$$\begin{pmatrix} \delta \dot{x}_{INS} \\ \delta \dot{x}_{GPS} \\ \delta \dot{x}_{SAR} \end{pmatrix} = \begin{pmatrix} F_{INS}(t) & 0 & 0 \\ 0 & F_{GPS}(t) & 0 \\ 0 & 0 & F_{SAR}(t) \end{pmatrix} \begin{pmatrix} \delta x_{INS} \\ \delta x_{GPS} \\ \delta x_{SAR} \end{pmatrix} + \begin{pmatrix} w_{INS} \\ w_{GPS} \\ w_{SAR} \end{pmatrix}$$

The following Table describes the total amount of truth model states used, depending upon GPS type. Case 1 refers to the stand-alone GPS, Case 2 refers to differential GPS, and Case 3 refers to carrier phase differential GPS.

Integrated Truth Model States			
	Case 1	Case 2	Case 3
INS	39	39	39
GPS	30	22	24
SAR	6	6	6
Total States:	75	67	69

Noise that the SAR model does not include the seven states.

The integrated filter model is represented in the same manner as the truth model. However, since the actual implementation of a Kalman filter truth model onboard an aircraft would take a tremendous amount of computational capability a filter model is used to represent the truth model using less states. The final result is a reduced order filter model that is more suited for online application of a Kalman filter on board aircraft. The following table describes the number of states used in the integrated filter for each GPS type.

INTEGRATED FILTER MODEL STATES			
	Case 1	Case 2	Case 3
INS	11	11	11
GPS	2	2	4
SAR	5	5	5
Total States	18	18	20

The original INS truth model contains 93 error states. The filter model is using the first 11 states. These 11 states comprise aircraft position error, velocity error,

misalignment errors, and barometric altimeter errors. Any further reduction of states from the 11-state filter model creates instabilities in the Kalman filter.

The stand-alone GPS truth model contains 30 error states. However, the most dominant states in the truth model are the user clock bias and drift states. These two states contribute an order of magnitude more error to the GPS pseudorange equation than the other error sources combined. Therefore the stand-alone GPS filter model can be reduced to just the user clock bias and drift states. The differential GPS filter model also contains only these two states. The CPGPS model contains a carrier-phase ambiguity state (per satellite) that is not necessary in the SGPS and DGPS models. Previous research has shown that the CPGPS filter model must include these states to remain stable across the entire flight profile. Therefore, the CPGPS filter contains an additional four states, which is not included in the SGPS and DGPS models. However, with the double differencing technique applied to the CPGPS model, the user clock bias and clock bias drift states are removed.

According to Maybeck, the filter may be unable to retain observability of the multiple random bias states in the SAR error model. Therefore, the 6-state truth model is condensed into a 5-state filter model, one state for range bias, one state for range rate bias, and three states for SAR target position errors. This technique will preserve the observability of each state while the state reduction can be tuned. Even with the state reduction, there are still additional random bias states remaining in the filter model. Further reduction of these states is necessary when developing a flight worthy Kalman filter for implementation and flight set.

The measurement models extend to each sensor measurement input into the integrated Kalman filter. There are four types of measurement available to the filter:

- Barometric altimeter
- Satellite pseudoranges
- SAR range and
- SAR range rate measurements

The baro and satellite measurements are available at 1Hz rates. The SAR measurements are available twice during a specific portion of the flight profile. This simulates the ability of a SAR to make a target range/range rate measurement, and

then be retasked for a second set of measurements during the reconnaissance mission. Two measurements are typical for a reconnaissance mission; however for a fighter targeting mission, several hundred measurements at a very high rate may be desirable. One change occurs in between the GPS simulations, that of the double difference in the CPGPS measurement model. This model produces only 3 measurements as opposed to the four pseudorange measurements in the SGPS and DGPS cases.

3 Simulation software

Several software packages used in this essay. Each package is vital to the complete Kalman filter simulation. MSOFE provides the simulation code for evaluating a Kalman filter design against a truth model. MPLOT produces complete data sets and Monte Carlo statistics of user-defined variables as generated MSOFE. PROFGEN compiles the flight profiles used in MSOFE to control the simulation. Together, these three software programs comprise the "AVLAB Toolbox" which defines the flight profile, runs the Kalman filter simulation and generates the complete data output. MATLAB is then used to analyze, plot and display all results.

4 Simulation Results

In previous research of AFIT relative to completion of INS / PST that is concentrated mainly in the validation standards and standards truth filters and accuracy approaching aircraft and in both cases, the type of flight pattern, except for the portion of the landing, there was critical for the actual research topic. However, the focus of this research was to simulate a typical reconnaissance mission of the U-2. A new layout flight was necessary to accomplish this objective leads to outline flight "U-2 flight". [1] contains a complete collection of plots charts covering the position of the "U-2Flight", speed, positioning, and the rate of placement over the entire flight profile.

The flight profile of U-2 is divided into 10 departments whose three parts are repeated twice to produce the flight path of the racetrack that lasts 3700 seconds.

While the flight profile is not a complete flight of the U-2 from takeoff to landing, sufficient for initial performance analysis of targeting, since the purpose of this

research is to determine the accuracy of the SAR addressing concerns over different types of receivers the GPS. Therefore, only the first 1200 seconds of the flight pattern analysis are discussed in sections below. The first 1200 seconds of the flight profile cover 20 minutes of the performance of Kalman filters and include both measurements of SAR.

The simulation results MSOFE are presented in each case ([1]). Starting from the SGPS, they are analyzed the errors of the position of aircraft and the accuracy of the location of targets embedded system INS / GPS / SAR. The result of this research is to determine the effects and affects different applications of GPS that can have on the targeting recognition of SAR. The results in each case are compared to determine the best theoretical results obtained through this research.

The average trace of error determined by the following equation:

$$\hat{M}_e(t_i) = \frac{1}{N} \sum_{i=1}^N e_j(t_i) = \frac{1}{N} \sum_{i=1}^N \{\hat{x}_{Filter\ j}(t_i) - \hat{x}_{True\ j}(t_i)\}$$

where $\hat{x}_{Filter\ j}(t_i)$ represents the filter is calculated and the standard error-state estimates truth at times t_i . N is the total number of runs of Monte Carlo for the simulation.

4.1 First case: The Standalone GPS

The flight profile "U-2Flight" was used to provide the elements of truth to simulate integrated system INS / GPS / SAR with SGPS.

The general effects of errors SGPS aircraft provided in the following Table.

SGPS Aircraft Errors			
Ave. Position (ft)	Latitude	Longitude	Altitude
	8.00	6.17	14.39
Ave. Velocity (ft/s)	North	East	Down
	0.18	0.25	0.53
Ave. Attitude (rad)	North	East	Down
	2.27E-5	5.74E-4	1.62E-5

Mid position errors were: 8.00 FT for latitudes, 6.17 FT for longitude and 14.39FT for height. The RMS value of the aircraft position error was 17.59 over 19 - FT found in previous research SGPS.

Looking at the source of error seems to be influenced by the accuracy and type of standard GPS, forcing the calculated filtered covariance propagate back to previous levels within triplicates. On the side of the speed measurement range SAR rate had a significant impact on error estimates from the north and down. There was also a secondary anomaly with consolidated SGPS system. Moreover, since the covariance filter does not reflect the same anomaly with the true error, the problem must be an anomaly in the model truth SGPS taken several steps to fix this problem, including running the filter without the standard SAR, coordination of noise measurement and process filters GPS, and the standard state reduction truth. Each of these methods, failed to correct the true slope error and increase the true covariance.

Adding the measurement consolidated filter Kalman INS / GPS provided a 13.21% reduction in the wrong geological targets. However, no other simulation uses a different standard GPS, it is impossible to determine whether this reduction is due to the accuracy or precision SAR aircraft position.

4.2 Second Case: The Differential GPS

The flight profile "U-2Flight" was used again to provide the elements of truth to simulate embedded system INS / GPS / SAR, this time using a simulated receiver DGPS.

The standards and INS SAR remained the same, comparing the case 1.

In this case, the average position errors were: 1.91 FT for latitudes, 1.87FT for longitude and 4.24 ft for height. The total aircraft position error RMS was 5.01 ft replicating the results of previous research.

Mistakes latitude and height aircraft show a decrease of 1 % calculated in filtered covariance over three seconds.

The unified DGPS provides very accurate estimates of position and speed of aircraft. The difference equations SAR measurements show a direct relationship between the measurements and errors aircraft position. If errors aircraft position disclosed accurately, the SAR measurements will produce a greater influence in the Member misplaced goals.

4.3 Third Case: GPS Phase Transfer

The blueprint flight "U-2 Flight" used at the end to provide the elements of truth to simulate embedded system INS / GPS / SAR, this time using the simulated receivers CPGPS. Regarding previous research using the model CPGPS, the embedded system has functioned better than expected, as the standard of DGPS.

The general results of CPGPS for errors aircraft are given in the next Table.

	CPGPS Aircraft Errors		
	Latitude	Longitude	Altitude
Ave. Position (ft)	2.04	1.55	2.02
Ave. Velocity (ft/s)	North	East	Down
	0.17	0.18	0.19
Ave. Attitude (rad)	North	East	Down
	1.34E-5	2.41E-4	1.16E-5

In this case, the errors in the position were: 2.04 - ft for latitude, 1.55-ft for longitude, and 2.02- ft for height. The total error of the position of aircraft RMS was 3.26 - ft performing slightly better than the previous survey. The errors of latitude and height of aircraft, like those in case 2, showing only smaller effects, a reduction of less than 1% in the calculated covariance filter over three seconds.

The standard CPGPS differs from the pattern of DGPS by adding the state of the 4- ambiguity integers filters standards and standards truth.

The results for the accuracy goals of CPGPS case can be found in the following Table.

	CPGPS Targeting Errors		
	X-Position	Y-Position	Z-Position
Initial Error (ft)	5.37	12.58	12.92
Final Error (ft)	2.05	9.85	5.13
Percent Decrease	61.74%	21.69%	60.27%

Using the same standard as in case SAR 1 and 2, the positioning accuracy decreases comparison in the previous measurement of RMS 18.81 ft in 11,29 ft. The reduction results in a 39.96 % increase in the accuracy RMS geological targets. X and

Z channels affected in most cases with an increased precision targeting 61.74 % and 60.27 %, respectively. The accuracy of channel Y - position increased by 21.69 %.

An important aspect of this study was to compare the performance of each case integrated INS / GPS / SAR.

The CPGPS provided the best accuracy positioning aircraft and targets. According to simulation results of error position aircraft and targets, the unified SGPS provided a 13.20% improvement on error geological targets after treatment two measurements SAR. The DGPS produced a 20.78 % improvement in the accuracy of geological targets while CPGPS provided an improved accuracy 39.96 %. And DGPS and CPGPS provided excellent aircraft stands, buggy RMS 5 FT or less. Using standard Tables ([1]) as a guide, the DGPS provided the greatest improvement in precision target location and also provided an enormous increase in positional accuracy aircraft against the liability of the SGPS. The CPGPS however had the lowest final total wrong target and the wrong aircraft and therefore had the best performance.

5 Conclusions

Each of the GPS receivers formed in this work shows an increase in precision targeting the embedded standard SAR. The main focus of this research was to determine the effect on aircraft position accuracy and precision is by its effect on SAR. With the simulation of three different systems and keeping the same model between the SAR, the improvements in targeting can be attributed to positional accuracy aircraft. While the accuracy of the SAR measurements provide the greatest means for improving the fusion of GPS measurements provide even greater improvement over the modification of the SAR. In reconnaissance aircraft SAR, the SAR measurements will be incorporated in the Kalman filter navigation to receive this additional benefit. Previous research by Layne studying the built SAR sensors and navigation produced high accuracy in measurements SAR, addressing the results.

The flight profile used in this study was sufficient to determine the theoretical performance of the integrated system INS / GPS / SAR. The system showed no performance degradation due to layout type specific flight. The positioning of the assimilated into the target folder performance standard SAR was very important.

Several attempts simulation failed because the target was outside the capabilities of the standard SAR.

The bottom line leads to this thesis focused on the benefits of targeting the SAR measurements in the Kalman filter navigation INS / GPS. This research has shown that there are performance gains by implementing the appropriate tight integration of sensor SAR. Beyond standard receivers GPS, which aims at improved results, CPGPS by almost 25%, simply by completing filters SAR Kalman. The function in a standalone option (i.e. no integration with INS / GPS) the SAR would not be able to achieve these benefits.

References

- [1] Brian, James Young, *An Integrated Synthetic Aperture Radar/Global Positioning System/Inertial Navigation System for Target Geolocation Improvement*, Ph.D. dissertation, AFIT/GE/ENG/99M-32, School of Engineering, Air Force Institute of Technology, Wright-Patterson AFB, OH, March 1999
- [2] Miller, Mikel M., *Modified Multiple Model Adaptive Estimation (M^3AE) for Simultaneous Parameter and State Estimation*. Ph.D. dissertation, AFIT/GE/ENG/98-02, School of Engineering, Air Force Institute of Technology, Wright-Patterson AFB, OH, March 1998
- [3] Maybeck, Peter S., *Stochastic Models, Estimation and Control, I*. New York: Academic Press, Inc., 1982
- [4] Musick, Stanton H. and Neil Carlson, *User's Manual for a Multimode Simulation for Optimal Filter Evaluation (MSOFE)*. Air Force Avionics Laboratory, Wright- Patterson AFB, OH, April 1990. AFWAL-TR-88-1138
- [5] Lewantowicz, Zdzislaw H. and Randall N. Paschall., "Deep Integration of GPS, INS, SAR, and Other Sensor Information," Proceedings of ION National Technical Meeting 1998

- [6] Layne, Jefferey R., *Integrated Synthetic Aperture Radar and Navigation Systems for Targeting Applications*. WL-TR-97-1185, Air Force Avionics Directorate, Wright- Patterson AFB, OH, September 1997
- [7] Kaplan, Elliott D., *Understanding GPS, Principles and Applications*. Boston: Artech House, Inc., 1996
- [8] Harger, Robert, *Synthetic Aperture Radar Systems, Theory and Design*. New York: Academic Press Inc., 1970
- [9] Ornedo, Renato S. and Farnsworth, Kenneth A., "GPS and Radar Aided Inertial Navigation System for Missile System Applications," Proceedings of ION National Technical Meeting 1998, Long Beach, CA, January 21-23, 1998
- [10] Abbott, Rich, "Synthetic Aperture Radar Location Accuracy Assessment," Lockheed Martin Skunkworks Interdepartmental Communication, ASC/RAP, Wright-Patterson AFB, OH, 8 May 1995
- [11] Grejner-Brzezinska, Dorota A., "Direct Platform Orientation with Tightly Integrated GPS/INS in Airborne Applications," Ohio State University Center for Mapping, Columbus, OH, 1998
- [12] Li, Rongxing, "A Study of Referencing Issues in Multi-Platform and Multi-Sensor Based Object Location," AFRL/SNAT, Wright-Patterson AFB, OH, 1998
- [13] Britting, Kenneth R., *Inertial Navigation Systems Analysis*. New York: Wiley- Interscience, 1971
- [14] Vasquez, Juan R., *New Algorithms for Moving-Bank Multiple Model Adaptive Estimation*. Ph.D. dissertation, AFIT/DS/ENG/98-10, School of Engineering, Air Force Institute of Technology, Wright-Patterson AFB, OH, May 1998
- [15] Vasquez, Juan R. *New Algorithms for Moving-Bank Multiple Model Adaptive Estimation*. Ph.D. dissertation, AFIT/DS/ENG/98-10,

School of Engineering, Air Force Institute of Technology, Wright-Patterson AFB, OH, May 1998.

- [16] Bohenek, Brian J. *The Enhanced Performance of an Integrated Navigation System in a Highly Dynamic Environment*. MS thesis, AFIT/GE/ENG/94D-01, School of Engineering, Air Force Institute of Technology, Wright-Patterson AFB, OH, December 1994.
- [17] Bagley, Daniel, T. *GPS/INS Integration for Improved Aircraft Attitude Estimates*. MS thesis, AFIT/GE/ENG/91D-04, School of Engineering, Air Force Institute of Technology, Wright-Patterson AFB, OH, December 1991.